

## DFT Study of the Formation of $\alpha$ -Chloro-Pyruvic Esters from $\alpha$ -Chloroglycidic Esters Isomers

Souad Jorio<sup>1\*</sup>, Hassna Abou El Makarim<sup>2</sup>, Mohamed Tabyaoui<sup>3</sup>

1. Chouaïb Doukkali University, Faculty of Science, Department of Chemistry, Molecular Modeling and Spectroscopy Team E2MS. BP20, 24000 El Jadida Morocco.
2. Mohammed V University, Faculty of Sciences, Department of Chemistry, LS3ME Team Theoretical Chemistry and Molecular Modeling. BP 1014 Avenue Ibn Batouta, Rabat, Morocco.
3. Mohammed V University, Faculty of Sciences, Department of Chemistry, Laboratory of Materials Nanoparticles and Environment, BP 1014 Avenue Ibn Batouta, Rabat, Morocco.

Received 13 Jan 2017,  
Revised 13 May 2017,  
Accepted 15 May 2017

### Keywords

- ✓ DFT;
- ✓  $\alpha$ -chloridrate glycidic esters;
- ✓ Chloro-pyruvics esters;
- ✓ NBO;
- ✓ Wiberg index

S Jorio  
[sjorio2000@yahoo.fr](mailto:sjorio2000@yahoo.fr)  
0673795351

### Abstract

In this work, we studied the ring opening mechanism of  $\alpha$ -chloroglycidic esters in the presence of Lewis acid  $MgCl_2$ . This reaction mechanism leads to the formation of chloro-pyruvic esters. Our theoretical study was carried out in the solvated phase using density functional theory at the B3LYP/6-31G (d) level. The geometric structures at the various stationary points on a part of this reaction path were fully optimized. The theoretical calculations of the different energy levels were in agreement with the experimental data. A study of the potential energy surface allowed to identify different molecular complexes associated with the approach reaction of the Lewis acid on the  $\alpha$ -chloro glycidic ester preceding the formation of the transition structures. In order to account for the molecular mechanism, we calculated the Wiberg index for the transition states and pyruvic products using natural bond orbital analysis (NBO). For a better interpretation of our reaction mechanism, we calculated the percentage of evolution of the bonds that break and form (% EV) along our chemical process. The results allowed to verify that the reaction mechanism is concerted, which is in good agreement with previous experimental results.

## 1. Introduction

The  $\alpha$ -halogenoglycidic esters were prepared from the dialdogalactose and the isopropyl di-halogenoacetate [1] according to the following (Fig.1). They present an excellent synthesis intermediate leading to the formation of the molecules of the pyruvic esters, which present a biological interest in metabolic processes [2, 3].

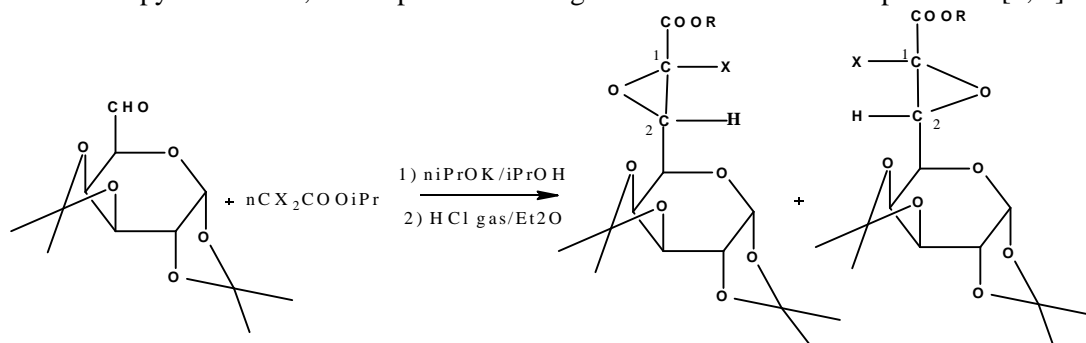


**Figure 1:** Formation of glycidic ester from dialdogalactose and the isopropyl di-halogenoacetate.

We focused our study on the understanding of the mechanism of the epoxy ring opening reactions of the  $\alpha$ -chloroglycidic ester [1] (Fig. 2) by the Lewis acid  $MgCl_2$  [2] which leads to the formation of chloro pyruvic esters [3] (Fig. 3).

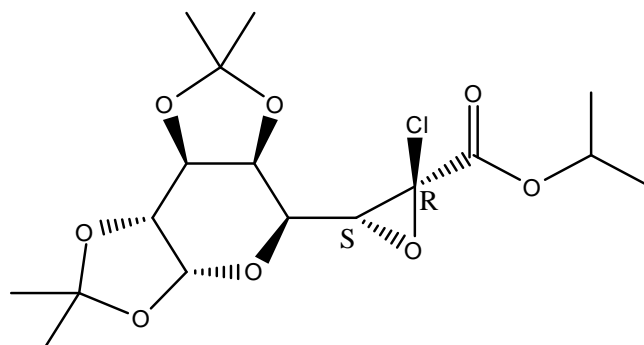


**Figure 2:** Structure of  $\alpha$ -chloroglycidic ester.

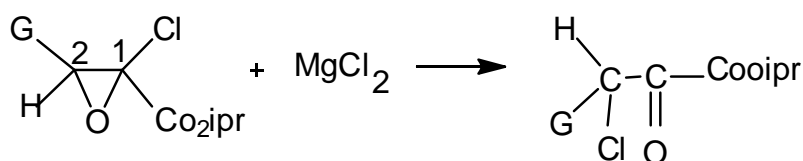


**Figure 3:** Reaction of  $\alpha$ -chloroglycidic ester with Lewis acid  $MgCl_2$  (G is relative to the glycidic group).

Experimentally, it has been demonstrated [1] that the  $\alpha$ -chloroglycidic ester (Fig .2) can give four diastereoisomers (2R,1S); (2S,1R); (2S,1S) and (2R,1R) [1]. The two cis diastereoisomers (2S,1S and 2R,1R) are more stable than the trans ones. The four diastereoisomers are presented in Figure 4.

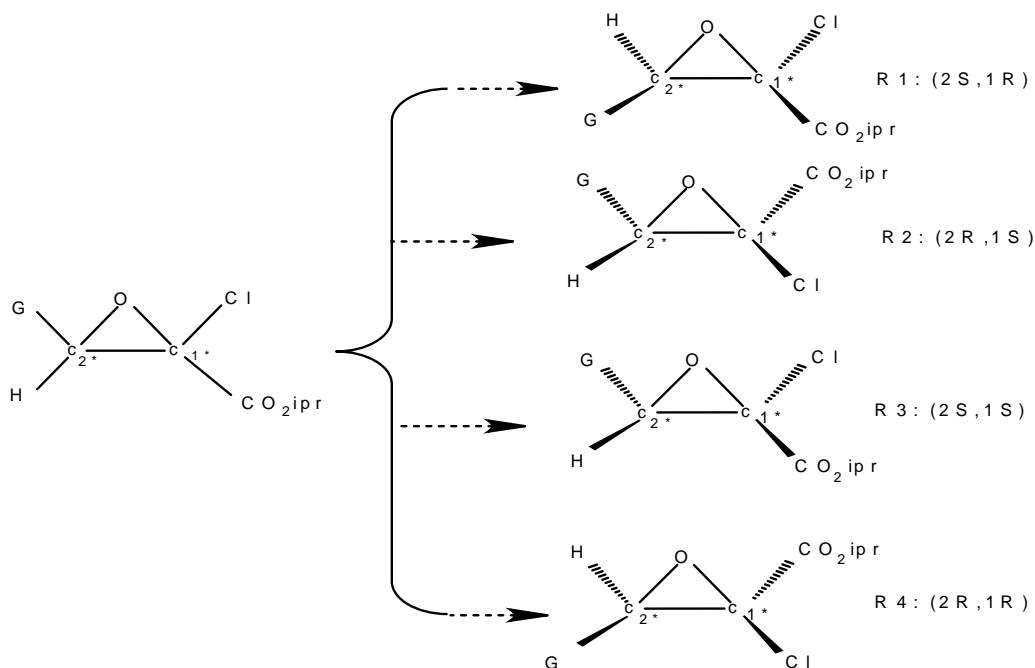


**Figure 4:** The four diastereoisomers of the  $\alpha$ -chloroglycidic ester.

## 2. Calculation methods

All calculations were performed with the program Gaussian 09 [4] and the results were visualized with Gauss View [5]. The calculations were done in tetrahydrofuran (THF) solution. The DFT method was used [6]. Several functional were tried: BPV86 [7], B3LYP [6] and PBEPBE [8]. Also four different basis sets were examined: 6-31G, 6-311G, 6-31G (d) and 6-311G (d, p) [9, 10-12].

We found that the functional B3LYP combined with the 6-31G (d) basis set is an adequate choice for our calculations. This functional allows a good description of all physicochemical parameters. In comparison with other functional, B3LYP yielded a similar precision while requiring less CPU time. B3LYP is a hybrid

functional which includes Becke's [6] gradient exchange correction and the Lee [13], Yang [13] and Parr [14] correlation functional.

The geometries were optimized by using the analytical gradient method of Berny [15, 16]. We also performed a vibrational frequency calculation in order to decide whether the geometry of the reactants, the molecular complexes or the products are a minimum [17,18] on the potential energy surface or a transition state [17,18], respectively. The optimized geometries of the transition states, however are characterized by one imaginary frequency which is associated to a single eigenvalue of the Hessian matrix [17, 18] and confirmed by an IRC calculation [19, 20].

The  $\alpha$ -chloroglycidic ester was studied using THF as a solvent and at the experimental temperature 323°K [1]. The solvent effect was studied by using the self consistent reaction field (SCRF) [21, 22-24] based on the polarizable continuum model PCM [21, 25-26]. A full optimization of the geometries in solution [26, 27-29] was done by using this model.

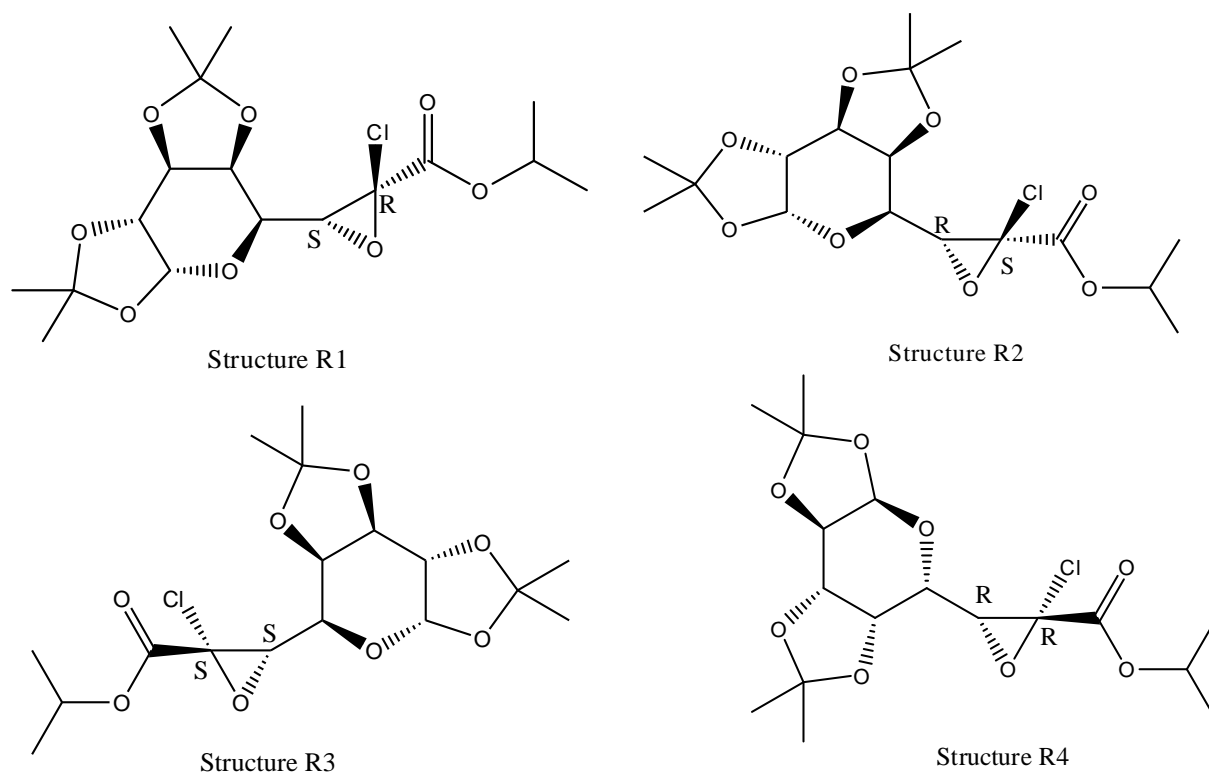
### 3. Results and Discussion

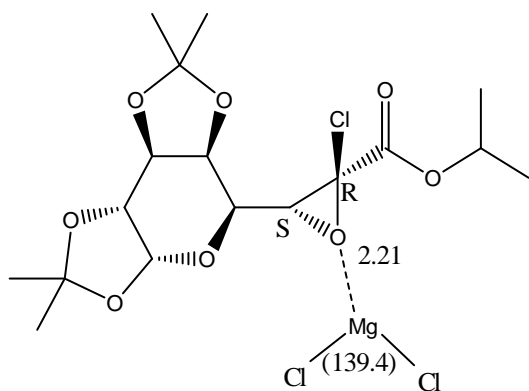
By exploring the potential energy surface we identified different molecular complexes (MC), depending on the approach of the reactants and the Lewis acid  $MgCl_2$  [2]. To describe the reaction path of the ring opening of the  $\alpha$ -chloroglycidic ester (Fig .3) in the presence of the Lewis acid  $MgCl_2$ , it is necessary to know the optimal geometries of the various stationary points on the reaction path. Therefore, we did a full structure optimization of the reactants, the molecular complexes, the transition states and the products.

The approach of Lewis acids has been realized theoretically on both sides of the epoxy ring of the  $\alpha$ -chloro glycidic ester [1], which leads to the formation of two chloro-pyruvic esters [3]. The energies of the molecular complexes were calculated at an interatomic distance equal to 4Å between the Lewis acid  $MgCl_2$  and the oxygen atom of the epoxy function. This energy was evaluated after the full optimization of our molecular system and followed by a vibrational frequency calculation of these molecular complexes. These are Van der Waals complexes [30, 31]. We found that these molecular complexes are more stable than the reactants.

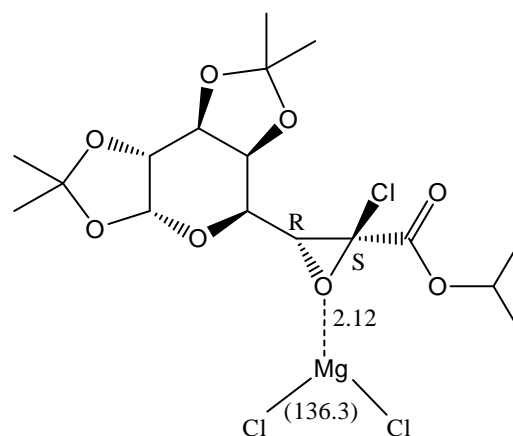
#### 3.1. Optimization of the reactants, the molecular complexes, transition states and products

In order to get deeper insight into the investigated process, we calculated the optimized geometries of all stationary points. We report below in Figure 5 the optimized structures of the reactants, the molecular complexes and the products in solution.

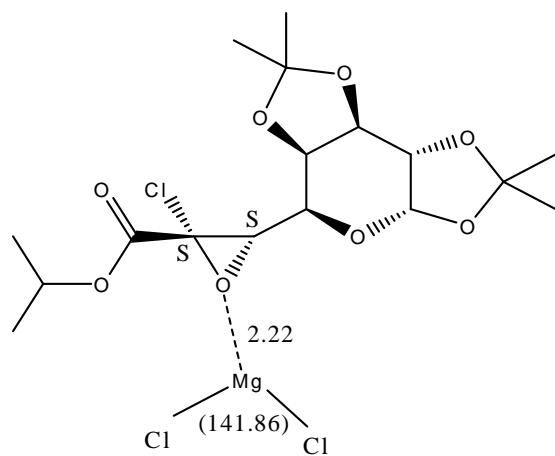




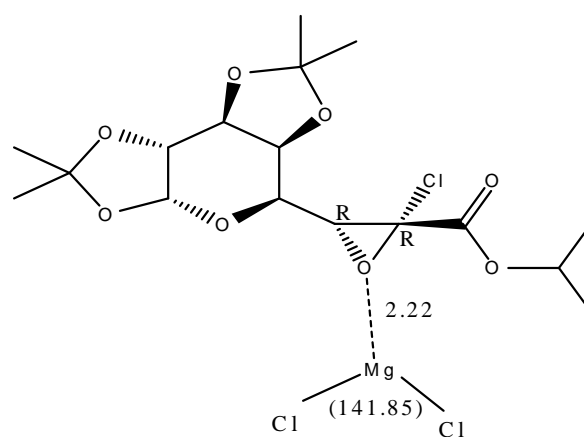
Structure MC1



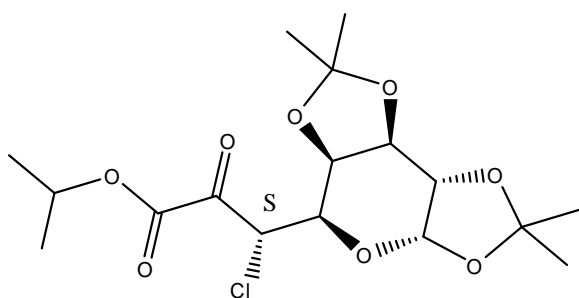
Structure MC2



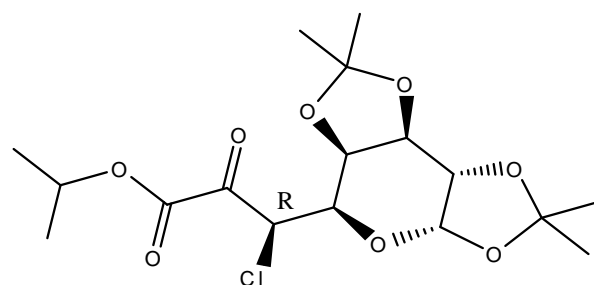
Structure MC3



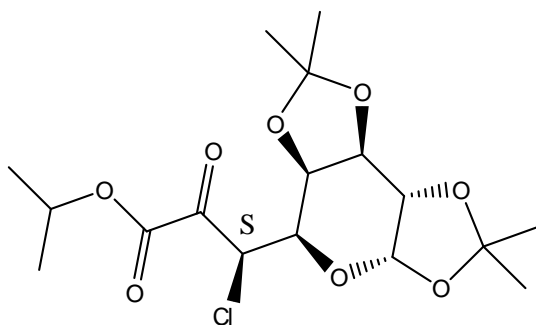
Structure MC4



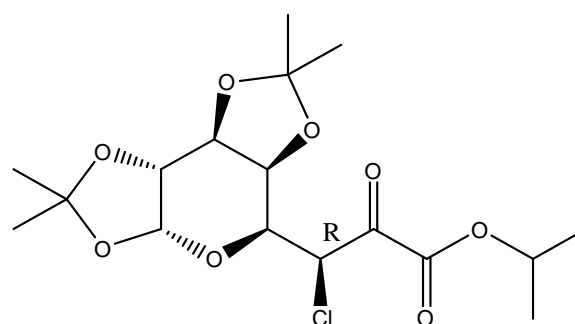
Structure P11



Structure P12



Structure P21



Structure P22

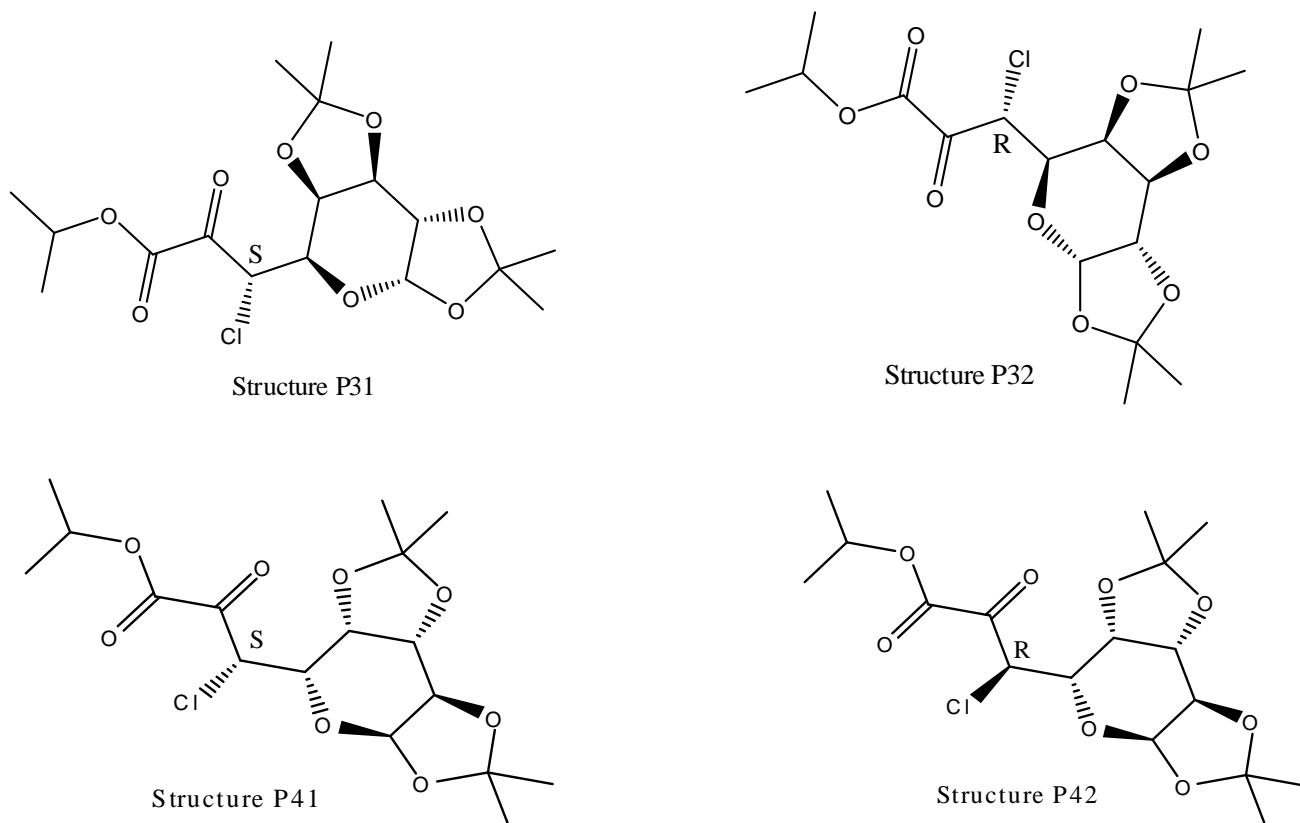


**Figure 5:** Optimized structures in solution for reactants, molecular complexes and products.

We note that the products (P11, P12); (P21, P22); (P31, P32) and (P41, P42) are the structures of chloro-pyruvic esters obtained from the diastereoisomers R1 (2S,1R); R2 (2R,1S); R3 (2S,1S) and R4 (2R,1R).

In Figure 6, we show the structure of the  $\alpha$ -chloroglycidic esters and in Table 1 we report the parameters of the optimum geometries for the diastereoisomers (2S,1R); (2R,1S); (2S,1S) and (2R, 1R) in THF solution corresponding to the structures R1; R2; R3 and R4.

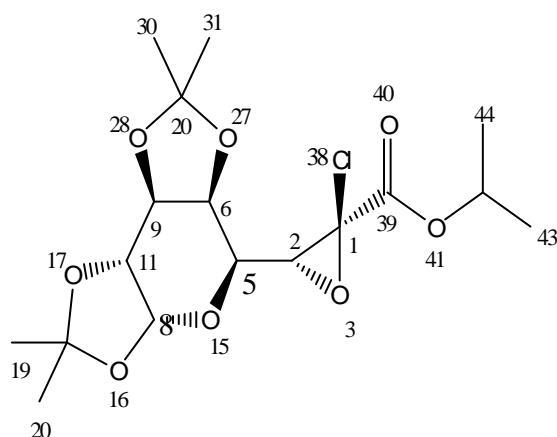


**Figure 6:** Structure of the  $\alpha$ -chloroglycidic esters optimized by the DFT method.

From the values in Table 1, we can deduce that:

- Bond lengths, angles of valence and dihedral angles are equal for the two configuration pairs (2R,1S); (2S,1R) and (2S,1S); (2R,1R) respectively.
- A full analysis of the structural parameters of the  $\alpha$ -chloroglycidic ester reveals that the geometry of the glycidic group is not affected by a structural change between the four configurations.

We can conclude that the optimal geometries do not differ significantly between the four diastereoisomers.

For the molecular complexes (MC1, MC2, MC3 and MC4), our theoretical calculations were performed in order to avoid the steric hindrance between the glycidic and the isopropyl groups. In the optimum configuration of the complex, we found that the distance  $d(\text{Mg}-\text{O})$  is equal to 2.12 Å for a configuration (2R,1S) and 2.22 Å for (2S,1R); (2S,1S) and (2R,1R) in solution. The optimum geometries are illustrated in Figure 5.

**Table 1:** Structural parameters of the four configurations of the  $\alpha$ -chloroglycidic ester in THF solution. Bond lengths are given in Angstroms, bond angles and dihedral angles in degrees

Parameters	(2S,1R)	(2R,1S)	(2S,1S)	(2R,1R)
$d(\text{C}_1-\text{Cl}_{38})$	1.806	1.806	1.793	1.794
$d(\text{C}_1-\text{O}_3)$	1.392	1.392	1.398	1.398
$d(\text{C}_2-\text{O}_3)$	1.465	1.465	1.447	1.447
$d(\text{C}_2-\text{C}_5)$	1.508	1.508	1.509	1.509
$d(\text{C}_5-\text{O}_{15})$	1.432	1.432	1.432	1.432
$d(\text{C}_6-\text{O}_9)$	1.552	1.552	1.552	1.553
$A(\text{C}_2-\text{C}_5-\text{H}_7)$	109.79	109.79	109.645	109.582
$A(\text{C}_2-\text{C}_1-\text{Cl}_{38})$	118.52	118.52	120.61	120.57
$A(\text{C}_2-\text{C}_5-\text{O}_{15})$	105.80	105.80	105.69	105.73
$A(\text{C}_2-\text{C}_1-\text{C}_{39})$	124.29	124.29	118.02	118.03
$A(\text{C}_2-\text{C}_6-\text{O}_{27})$	110.13	110.13	111.27	110.16
$A(\text{H}_4-\text{C}_2-\text{C}_5)$	115.15	114.15	115.30	115.17
$A(\text{O}_3-\text{C}_2-\text{C}_5)$	116.74	116.74	117.28	117.24
$D(\text{O}_3-\text{C}_2-\text{C}_5-\text{H}_7)$	38.32	-38.33	35.30	-35.17
$D(\text{H}_4-\text{C}_2-\text{C}_5-\text{H}_7)$	175.02	-175.02	173.18	-173.08
$D(\text{H}_4-\text{C}_2-\text{C}_5-\text{O}_{15})$	56.28	-56.29	54.547	-54.400
$D(\text{C}_2-\text{C}_5-\text{C}_6-\text{C}_9)$	157.67	-157.67	157.77	-157.96

### 3.2 Structure of the transition state

#### 3.2.1. Analysis of the geometric structures of the transition states and the evolution of the bond length on the reaction path

Our study was focused on the concerted mechanism of the epoxy ring opening reactions of the  $\alpha$ -chloro glycidic ester synthesized in the experiment [1]. In such a concerted mechanism, the chlorine atom of the Lewis acid  $\text{MgCl}_2$ , attacks the carbon atom. This leads to the opening of the epoxy ring and the departure of the chlorine atom in according to the scheme presented in Figure 7.

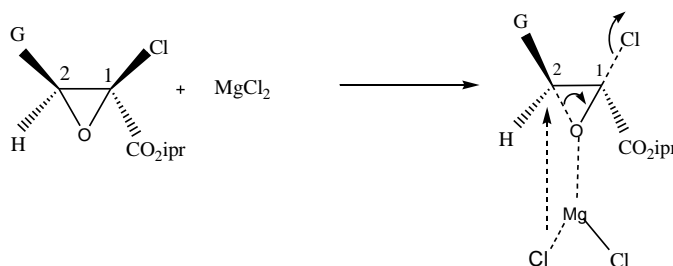


**Figure 7:** Scheme of the concerted mechanism.

The optimum geometries obtained in our study are almost the same for all the transition states. They have the form of an alkoxide.

The Figures 8, 9, 10, 11 summarize all the structures of the transition states in THF solution TS11; TS21; TS31; TS41, which lead to the "S" configuration of the chloropyruvic ester. However, TS12; TS22; TS32; TS42 lead to the chloro-pyruvic ester with an "R" configuration.

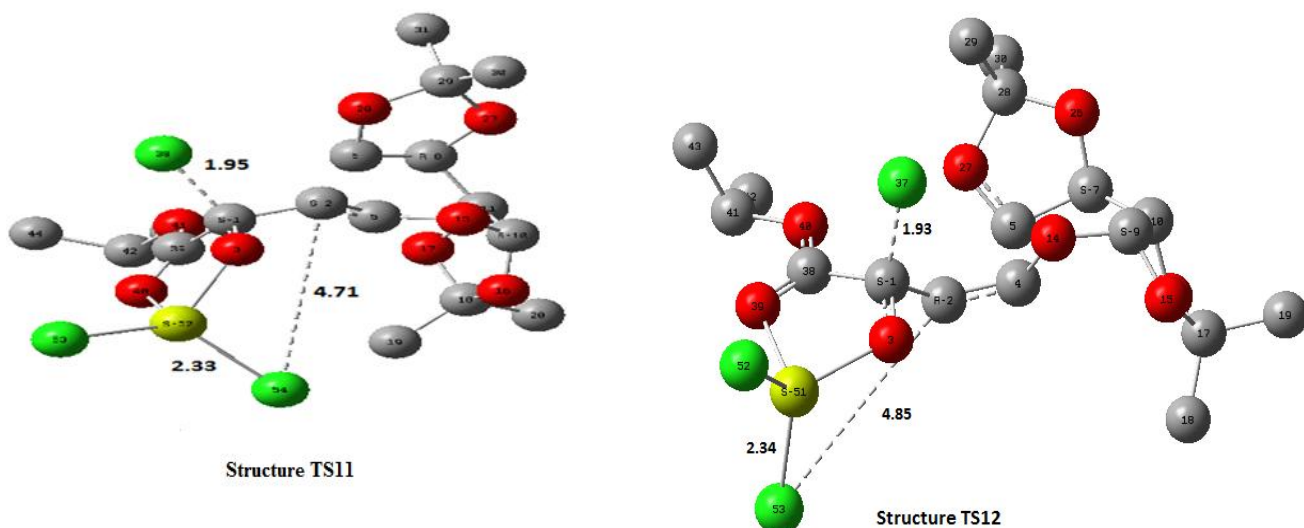


**Figure 8 :** Structure of the transition state TS11 and TS12 in THF solution calculated by B3LYP/6-31G (d).

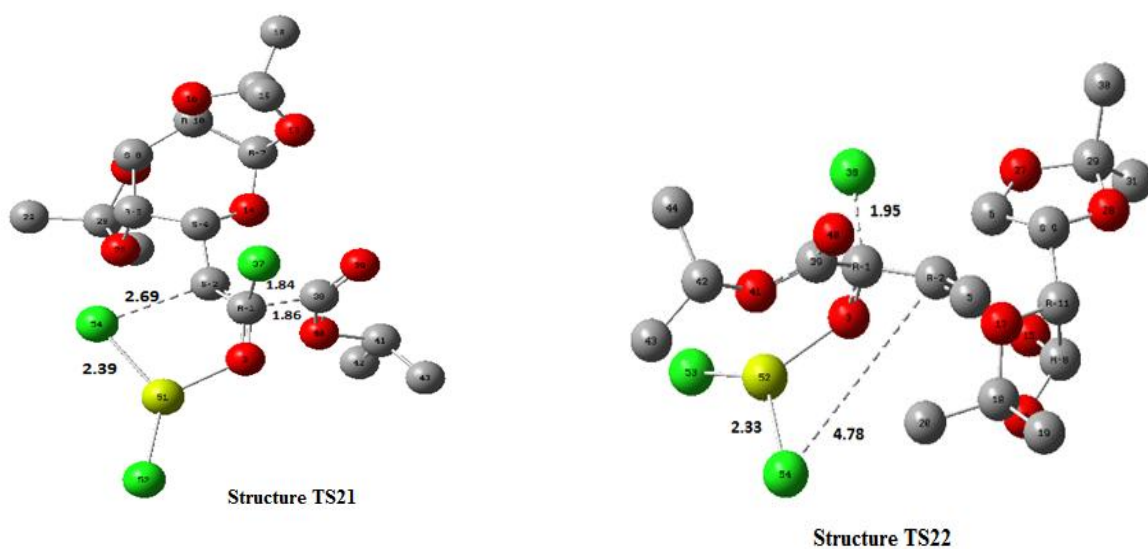


**Figure 9:** Structure of the transition state TS21 and TS22 in THF solution calculated by B3LYP/6-31G (d).

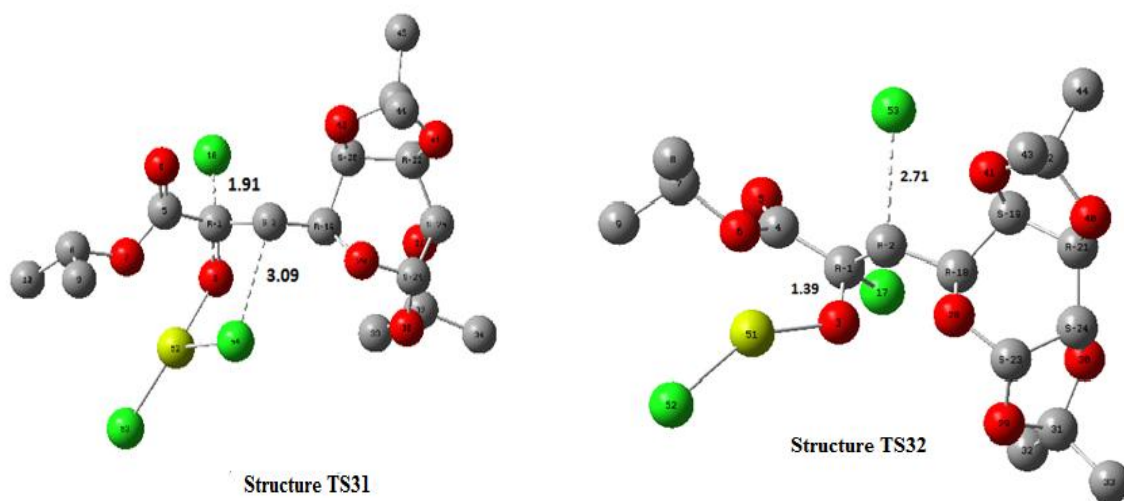


**Figure 10:** Structure of the transition state TS31 and TS32 in THF solution calculated by B3LYP/6-31G (d).

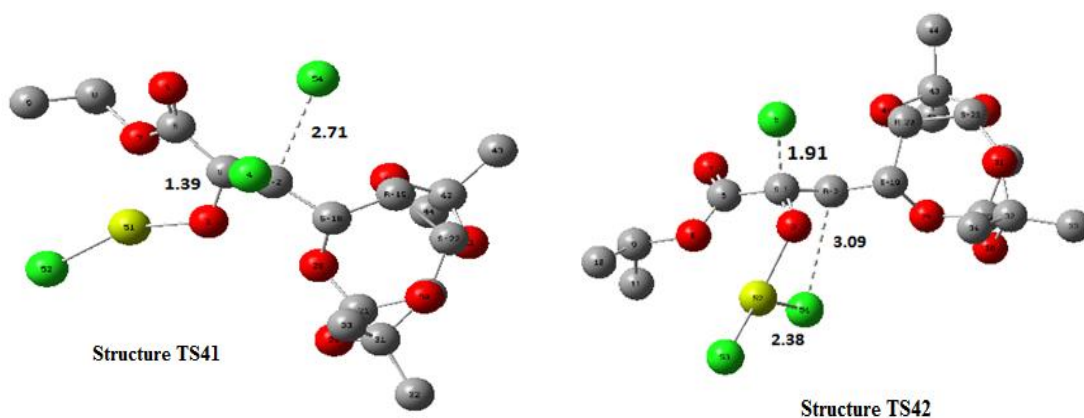


**Figure 11:** Structure of the transition state TS41 and TS42 in THF solution calculated by B3LYP/6-31G (d).

The structures of the transition state TS11; TS12; TS21 and TS22 obtained from the configurations (2S,1R) and (2R,1S) undergo bond breaking and they cannot lead to the chloro-pyruvic ester. Thus, the only states to consider are the transition states from the configurations (2S, 1S) and (2R, 1R). This result is in good agreement with previous work of Titov et al. [1], which showed that only two cis isomers for  $\alpha$ -chloroglycidic ester are obtained in Darzens reaction [1]. This will be explained below in our calculations.

We report in Table 2 some inter-atomic distances for the transition states in THF solution which lead to the chloro-pyruvic ester with an "S" and an "R" configuration of the asymmetric carbon.

**Table 2:** Interatomic ( $\text{\AA}$ ) distances for the transition states in THF solution

	TS31 (2S,1S)	TS32 (2S,1S)	TS41 (2R,1R)	TS42 (2R,1R)
C <sub>1</sub> -Cl <sub>38</sub>	1.91	1.78	1.78	1.91
C <sub>2</sub> -Cl <sub>54</sub>	3.09	2.71	2.71	3.09
C <sub>1</sub> -O <sub>3</sub>	1.31	1.39	1.39	1.31
C <sub>2</sub> -O <sub>3</sub>	2.20	1.75	1.74	2.44
Mg-Cl <sub>54</sub>	2.38	5.35	5.40	2.20
Mg-O <sub>3</sub>	2.22	2.20	2.22	2.00

From Table 2 we can see that:

- The interatomic distances are equal respectively for TS31; TS42 and TS32; TS41. We can explain this by the fact that the structures are enantiomers respectively.
- The interatomic distance C<sub>2</sub>-O<sub>3</sub> is higher in the transition states TS31 and TS42 than in reactants (1.44 $\text{\AA}$ ) indicating a ring opening of the epoxy. The O<sub>3</sub> atom is detached and favors the formation of a ketone bond. In fact, the bond length C<sub>1</sub>-O<sub>3</sub> decreases from the reactants (1.39  $\text{\AA}$ ) to the transition state (1.31  $\text{\AA}$ ).
- For C<sub>1</sub>-Cl<sub>38</sub>, the inter-atomic distance increases in the transition state. We can conclude that the chlorine is a leaving atom.

We present below the inter-atomic distances for all stationary points in the reaction process. We choose the cis-diastereoisomers path (2S, 1S) because this configuration is more stable than (2R, 1R) in solution. At the same time, we want to compare our theoretical mechanisms of the transition state with the previous results found by Coutrot et al. [2, 3].

We note that the bond length C<sub>2</sub>-Cl<sub>54</sub> decreases from the reactants to the products and the bond length Mg-Cl<sub>54</sub> increases. For C<sub>1</sub>-Cl<sub>38</sub> the bond length increases progressively in the reaction path. From the previous remarks, we can conclude that the isomerization of the  $\alpha$ -chloroglycidic ester with a Lewis acid takes place in two steps:

Step 1 - The formation of the molecular complex.

Step 2 - Passing through a transition state in the form of an alkoxide and attack of the chlorine atom from the Lewis acid on the carbocation in the C<sub>2</sub> position of the glycidic ester.



**Table 3:** Interatomic distances for the transition state TS31 (2S,1S) on the potential energy surface

d(Å)	Reactants R3	Molecular Complex MC3	Transition state TS31	Pyruvic ester P31(S)
C <sub>2</sub> -Cl <sub>54</sub>	-----	3.64	3.09	1.83
C <sub>1</sub> -Cl <sub>38</sub>	1.79	1.76	1.91	-----
C <sub>1</sub> -O <sub>3</sub>	1.39	1.42	1.31	-----
C <sub>2</sub> -O <sub>3</sub>	1.46	1.47	2.20	-----
Mg-Cl <sub>54</sub>	-----	2.32	2.38	-----

To confirm our results, we analyze the degree of lengthening of the two bonds that are breaking in the TS31 to obtain the percentage  $P_{(l)}$  of bond lengthening [32] between the transition state TS31 and the reactants R3, where the percentage of bond lengthening is given by:

$$P_{(l)} = \frac{l_{TS} - l_R}{l_R}$$

We found that the PI (C<sub>2</sub>-O<sub>3</sub>) (PI =51%) is more important than the PI (C<sub>1</sub>-Cl<sub>38</sub>) (PI =7%). We can say that the breaking of the bond C<sub>2</sub>-O<sub>3</sub>, is more advanced than the breaking of the bond C<sub>1</sub>-Cl<sub>38</sub>. From all these results, we can conclude that our reaction may be a concerted mechanism. We will verify that by an analysis of the Wiberg index [33].

### 3.2.2. Analysis of bond orders in the transition state

To find the bond types which form in the reaction process, the Wiberg index [33] has been calculated using the natural bond orbital analysis NBO [33] included in the Gaussian 09 program package [5]. In Table 4, we summarize the Wiberg bond indices corresponding to the bonds involved in the reaction leading to the "S" and "R" chloro-pyruvic ester respectively.

The process of bond breaking and bond forming along the reaction path can be analyzed employing the synchronicity index ( $S_y$ ) given by the formula of Moyano et al. [34].

$$S_y = 1 - \frac{\sum_{i=1}^n \frac{|\delta B_i - \delta B_{av}|}{\delta B_{av}}}{2n - 2}$$

where n is the number of bonds directly involved in the reaction and  $\delta B_i$  is the relative variation of the Wiberg bond index which is calculated as:

$$\delta B_i = \frac{B_i^{TS} - B_i^R}{B_i^P - B_i^R}$$

R, TS and P refer to reactants, transition states and products respectively. The average value  $\delta B_{av}$  is obtained from:

$$\delta B_{av} = n^{-1} \sum_{i=1}^n \delta B_i$$

The percentage of evolution (% EV) [33] of the bond order is calculated as: %EV= 100 $\delta B_i$ . Thus, ( $S_y$ ) is unity for a fully synchronous process and zero for a fully asynchronous process.

Our theoretical results for the cis-diastereoisomers (2S,1S) and (2R,1R) are presented below. This mechanism shows a synchronicity value of 0.80. The calculated Wiberg bond index along the reaction coordinate indicates that the C<sub>2</sub> - O<sub>3</sub> bond breaking (75.3%) occurs before the C<sub>2</sub> - Cl<sub>54</sub> (16.5%) and C<sub>1</sub> - Cl<sub>38</sub> (16.3%) which is the bond forming in our reaction.

**Table 4:** Wiberg bond indices ( $B_i$ ) of reactant, transition state TS31 and product in the process (2S,1S) or (2R,1R), percentage of evolution (%EV) of the bond order at the transition state, degree of advancement state ( $\delta B_{av}$ ), and absolute synchronicities  $S_y$ . Values obtained at B3LYP/6-31G(d)

	C <sub>1</sub> -O <sub>3</sub>	C <sub>2</sub> -O <sub>3</sub>	Mg-O <sub>3</sub>	Mg-Cl <sub>54</sub>	C <sub>2</sub> -Cl <sub>54</sub>	C <sub>1</sub> -Cl <sub>38</sub>
$B_i^R$	0.98	0.97	0.00	0.00	0.00	0.98
$B_i^{TS}$	1.15	0.24	0.18	0.40	0.16	0.82
$B_i^P$	1.84	0.00	0.00	0.00	0.97	0.00
%EV	19.77	75.26	----	----	16.49	16.33
$\delta B_{av}$	0.213					
$S_y$	0.80					

### 3.2.3. Atomic charge densities of the transition state

The charge distribution of the reactants and the transition state as obtained by the NBO analysis [32,33] is given in Table 5. It can be seen that the positive charge on C<sub>2</sub> increases significantly in the transition state as well as the negative charges on Cl<sub>38</sub> and O<sub>3</sub>.

**Table 5:** Atomic charge densities in the reactant R3 and in the transition state TS31

Atoms	C <sub>1</sub>	C <sub>2</sub>	O <sub>3</sub>	Cl <sub>38</sub>	Cl <sub>54</sub>	Mg
R3 (2S,1S)	0.14	0.07	-0.49	-0.03	-----	----
TS31(S)	0.19	0.18	-0.75	-0.11	-0.64	1.28

These results reveal that our mechanism occurs in two steps:

Step 1: A ring opening of the epoxy group and formation of a carbocation on C<sub>2</sub>.

Step 2: Attack of the chlorine atom Cl<sub>54</sub> from the Lewis acid on the carbocation C<sub>2</sub> and departure of Cl<sub>38</sub>.

## 4. Study of the reaction mechanism between the $\alpha$ -chloroglycidic ester and the Lewis acid MgCl<sub>2</sub>

### 4.1. Energetic aspect of the isolated species in THF solution

Our energetic study was realized in solution with THF as solvent at a temperature of 323°K, which is the same as the experiment [1]. The calculations were done according to the concerted mechanism proposed in our study (Fig. 7). We report in Table 6 the energetic results for the isolated species.

**Table 6:** Energetic values in (a. u) of isolated species in THF solution

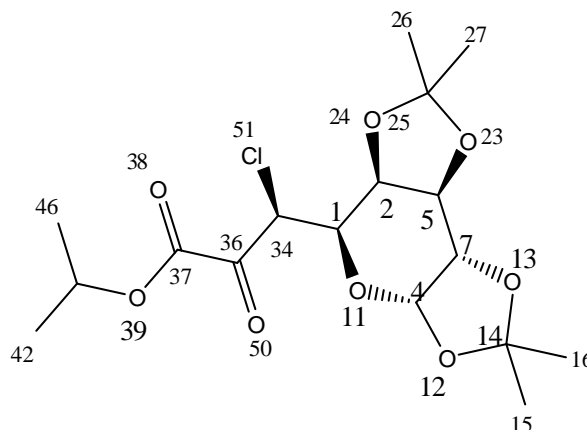
	Structure R <sub>1</sub> (2S,1R)	Structure R <sub>2</sub> (2R,1S)	Structure R <sub>3</sub> (2S,1S)	Structure R <sub>4</sub> (2R,1R)
Glycidic ester	-1724.824234	-1724.824233	-1724.825174	-1724.825089
MgCl <sub>2</sub>	-1120.682118			
	P11	P12	P31	P41
Pyruvic ester (S)	-1724.854548	-1724.858304	-1724.858318	-1724.851663
	P12	P22	P32	P42
Pyruvic ester (R)	-1724.847938	-1724.852905	-1724.851764	-1724.852905

Table 6, shows that the cis-diastereoisomers (2S,1S) and (2R,1R) are more favored thermodynamically than the trans-diastereoisomers (2S,1R) and (2R,1S) and the approach of the Lewis acid on the structure R<sub>3</sub> (2S,1S) leads to the chloro-pyruvic ester with configuration "S". For the structure R<sub>4</sub> (2R,1R), the chloro-pyruvic ester P<sub>42</sub> with configuration "R" is more stable than P<sub>41</sub>. The products P<sub>32</sub> and P<sub>41</sub> are isoenergetic. They represent the chloro-pyruvic esters obtained from the approach of Lewis acids on the "R" side of the epoxy ring of the diastereoisomer (2S,1S) and on the "S" side of the epoxy ring of the diastereoisomers (2R,1R), respectively. These structures are less stable compared to P<sub>31</sub> and P<sub>42</sub> because of the steric hindrance of the glycidic group with Lewis acids MgCl<sub>2</sub>.

At the same time, by an analysis of the energy of the structure **P31** and **P42**, we note that the structure **P31** is more stable than **P42**, so the conformation of the asymmetric carbon in the chloro-pyruvic esters is "S", it corresponds to the product **P31**.

All this permits the conclusion that our theoretical study is in good agreement with the experiment [35]. It has been confirmed by C-13 NMR that the cis-diastereoisomers are more stable than the trans-diastereoisomers [2,3] and the conformation of the asymmetric carbon in the chloro-pyruvic esters is an "S" [2,3].

We report in Figure 12 the optimum geometry for the chloro-pyruvic ester in THF solution **P31**. Some parameter values obtained in our theoretical calculations are shown in Table 7.



**Figure 12:** Optimized structure of chloro-pyruvic ester **P31** in THF solution.

**Table 7:** Structural parameters of the optimum geometry of chloro-pyruvic ester **P31** in solution

Bond length (Å)		Valence angle (degrees)		Dihedral angle (degrees)	
C <sub>34</sub> -Cl	1.83	Cl <sub>51</sub> -C <sub>34</sub> -C <sub>1</sub>	111.05	O <sub>11</sub> -C <sub>1</sub> -C <sub>34</sub> -Cl <sub>51</sub>	-62.30
C <sub>36</sub> -O <sub>50</sub>	1.21	Cl <sub>51</sub> -C <sub>34</sub> -C <sub>36</sub>	104.44	O <sub>11</sub> -C <sub>1</sub> -C <sub>34</sub> -C <sub>36</sub>	-179.85
C <sub>34</sub> -C <sub>1</sub>	1.52	C <sub>34</sub> -C <sub>36</sub> -O <sub>50</sub>	123.45	Cl <sub>51</sub> -C <sub>34</sub> -C <sub>1</sub> -C <sub>2</sub>	177.57
C <sub>1</sub> -O <sub>11</sub>	1.43	C <sub>34</sub> -C <sub>1</sub> -O <sub>11</sub>	106.46	C <sub>2</sub> -C <sub>1</sub> -C <sub>34</sub> -C <sub>36</sub>	60.02

The geometries for chloro-pyruvic ester in solution are similar for all diastereoisomers, except for the dihedral angles. We can explain this by the presence of single bond **C<sub>1</sub> - C<sub>34</sub>** allowing to rotate around this bond.

#### 4.2. Thermodynamic study of the reaction mechanism between $\alpha$ -chloridroglycidic ester and Lewis acid $MgCl_2$

In Table 8, we summarize several thermodynamic quantities characterizing the approach of  $MgCl_2$  to the  $\alpha$ -chloroglycidic esters **R3** and **R4** in THF solution.

**Table 8:** Thermodynamic quantities characterizing the approach of  $MgCl_2$  to  $\alpha$ -chloroglycidic ester in THF solution calculated by B3LYP/6-31G (d)

Reactants	Products	$\Delta H$ (kcal/mol)	$\Delta S$ (kcal/mol)	$\Delta G$ (kcal/mol)
R3(2S,1S)	P <sub>31</sub> (S)	-20.39	0.002	-21.12
	P <sub>32</sub> (R)	-16.43	0.003	-17.46
R4(2R,1R)	P <sub>41</sub> (S)	-16.35	0.003	-17.21
	P <sub>42</sub> (R)	-17.17	0.010	-17.56

The negative enthalpy and the Gibbs free energy show that the reaction is exothermic and thermodynamically possible and leads to two configurations "S" and "R". The ring opening of cis-diastereoisomers (2S,1S) lead to the chloro-pyruvic "S" which is more stable than "R". This can be confirmed by an analysis of the Gibbs free

energy, which amounts to -21.12 kcal/mol for the product "S" and -17.56 kcal/mol for the product "R". Our theoretical studies are in good agreement with the experiment [1].

### 5. Analysis of the potential energy surface and prediction of the reaction mechanism in THF solution

In Table 9, we report the energies corresponding to the cis and trans diastereoisomers of the  $\alpha$ -chloroglycidic ester, the energies of the molecular complexes as well as the energies of the transition states ETS(S) and ETS(R). Table 9 also shows the relative energy, which leads to the formation of the two chloro-pyruvic esters with the configuration "S", or "R" in THF solution, respectively. We also summarize the associated imaginary frequencies ( $\nu_i$ ). The potential energy profile for this reaction is shown in Figure 13.

**Table 9:** Transition state energies ETS(S), ETS(R), relative energy  $E_r$  and associated imaginary frequencies ( $\nu_i$ ) in THF solution

	<b>TS1</b> Path (2S,1R)	<b>TS2</b> Path (2R,1S)	<b>TS3</b> Path (2S,1S)	<b>TS4</b> Path (2R,1R)
	<b>P11</b>	<b>P21</b>	<b>P31</b>	<b>P41</b>
$E_{\text{products}}^{\text{S}}$ (a.u.)	-2845.536666	-2845.540422	-2845.540436	-2845.533781
	<b>P12</b>	<b>P22</b>	<b>P32</b>	<b>P42</b>
$E_{\text{products}}^{\text{R}}$ (a.u.)	-2845.530056	-2845.535023	-2845.533882	-2845.535023
	<b>R1</b>	<b>R2</b>	<b>R3</b>	<b>R4</b>
$E_{\text{reactants}}$ (a.u.)	-2845.506352	-2845.506351	-2845.507292	-2845.507207
	<b>MC1</b>	<b>MC2</b>	<b>MC3</b>	<b>MC4</b>
$E_{(\text{MC})}$ (a.u.)	-2845.521425	2845.521393	-2845.522495	-2845.522138
$\Delta E_{\text{S CM}}$ (kcal/mol)	-9.46	-9.44	-9.54	-9.37
	<b>TS11</b>	<b>TS21</b>	<b>TS31</b>	<b>TS41</b>
ETS(S) (a.u.)	-2845.496011	-2845.479969	-2845.481899	-2845.468090
$\nu_i$ ( $\text{cm}^{-1}$ )	205i	-359.72i	227i	385.19i
$E_r$ (kcal/mol)	6.49	16.55	15.93	24.55
	<b>TS12</b>	<b>TS22</b>	<b>TS32</b>	<b>TS42</b>
ETS(R) (a.u.)	-2845.489524	-2845.488004	2845.467735	-2845.481899
$\nu_i$ ( $\text{cm}^{-1}$ )	205.30i	122.85i	376i	227i
$E_r$ (kcal/mol)	10.56	11.51	24.82	15.88

i= imaginary frequency

As we stated before, we only consider the transition states which occur in the reaction starting from the cis-diastereoisomers (2S,1S) and (2R,1R) because in the trans diastereoisomers (2S,1R) and (2R,1S), the transitions states undergo bond breaking. Thus cannot lead to the corresponding chloro-pyruvic esters.

We note that the all transition states are characterized by one imaginary frequency in the Hessian matrix and the energy difference between  $\Delta E(\text{TS31}-\text{TS32})$  and  $\Delta E(\text{TS41}-\text{TS42})$  is almost the same because the transition states (TS31; TS42) and (TS32; TS41) are enantiomers.

At the same way, the chloro-pyruvic ester with configuration "S" **P31** is more stable than the chloro-pyruvic ester "R". Our theoretical results realized with DFT methods are in good agreement with the previous study of Tabyaoui [35], which showed by X-rays diffraction that the chloro-pyruvic ester with configuration "S" is more stable. However, the product **P31** is favored thermodynamically over the product **P42** and the energy gap between these two conformers is  $\Delta E=2.35$  kcal/mol. We conclude that the chloro-pyruvic ester **P31** with conformation "S" is the thermodynamic product and **P42** with conformation "R" is the kinetic product.

The energy profile in Figure 13 shows that the relative energy of TS42 (R) is lower than the relative energy of TS31(S). This implies that the product **P42** is forming first.

Table 10 summarizes the relative energies of the transition states TS31, TS32, TS41, TS42 and the stabilization energies of the products. It also shows that we have an early transition state, which is characteristic of exothermic reactions [36].

**Table 10:** Relative energies in kcal/mol of the transition states and the stabilization energies of the products

E(kcal/mol)	Conformation (2S,1S)		Conformation (2R,1R)	
$E_r$	<b>TS31</b>	<b>TS32</b>	<b>TS41</b>	<b>TS42</b>
	15.93	24.82	24.55	15.88
$E_s$	<b>P31</b>	<b>P32</b>	<b>P41</b>	<b>P42</b>
	-20.80	-16.68	-16.67	-17.45

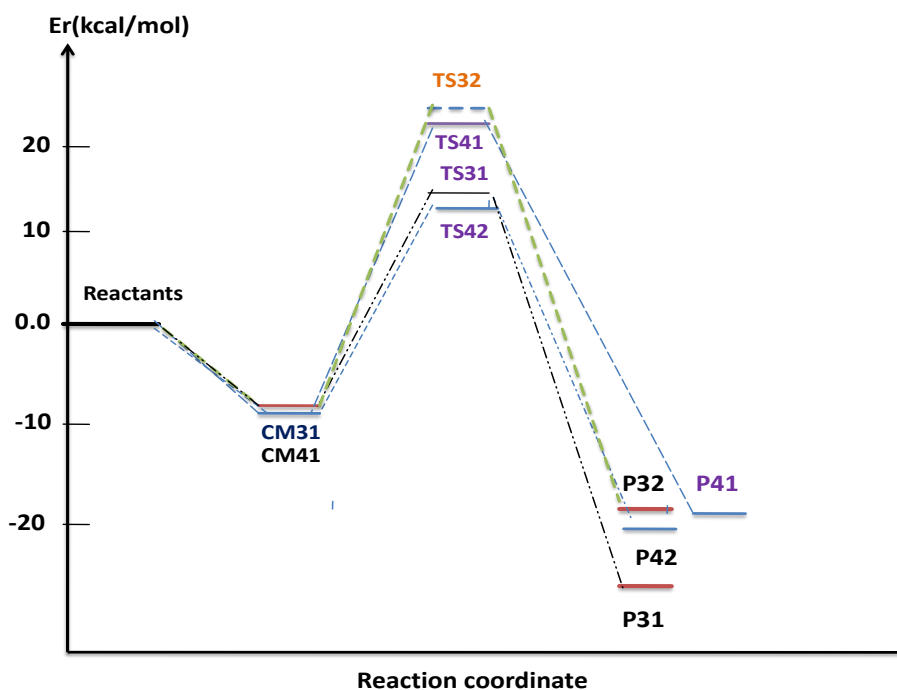


**Figure 13:** Energy profile of the reaction between  $\alpha$ -chloroglycidic esters and the Lewis acid in THF solution.

In order to check that the energy profiles connect the transition state TS31 with the two minima of the proposed mechanism, we performed an IRC calculation using the Gonzalez-Schlegel integration method [19,20]. In Figure 14, we present the curve  $E = f(\text{IRC})$  on both sides.

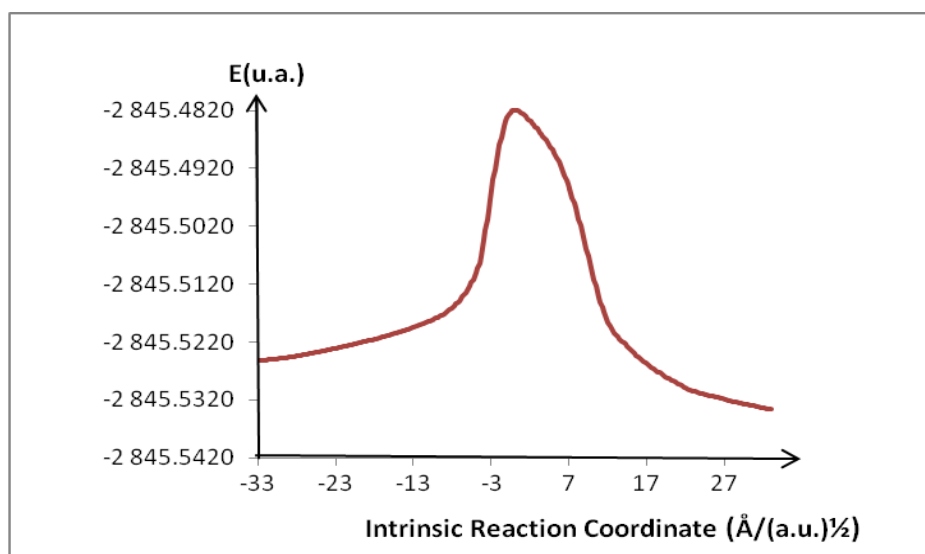


**Figure 14 :** IRC of the reaction between the  $\alpha$ -chloroglycidic ester with configuration (2S,1S) and  $\text{MgCl}_2$  calculated by DFT/B3LYP/6-31G (d).

Figure 14 shows that the transition state TS31 is well linked to the minima of the molecular complex MC3 and the product P31.

## Conclusion

In our study, we describe the reaction path of the ring opening of the glycidic esters in the presence of the Lewis acid  $\text{MgCl}_2$  in THF solution. The  $\alpha$ -chloroglycidic esters are the precursors of the most interesting pyruvic derivatives intervening in the metabolic processes and leading to the formation of biological molecules such as lipids.

Our theoretical results show that the cis-diastereoisomers of the  $\alpha$ -chloroglycidic ester and the chloro-pyruvic ester with configuration "S" are respectively more stable than the trans diastereoisomers and the chloro-pyruvic ester with configuration "R". These results are in good agreement with the experiment. At the same way, we located different molecular complexes, which correspond to Van der Waals complexes and which are more stable than the reactants.

The study of the transition state was realized on both sides of the epoxy ring of the  $\alpha$ -chloroglycidic ester and it is characterized by one imaginary frequency in the Hessian matrix. The IRC calculations were performed to show that the transition state is linked to the minima of the molecular complexes and the products.

To confirm the nature of the mechanism of our reaction, we made an analysis of the interatomic distances of the reactants and the transition states, which indicates that our reaction may be a concerted mechanism. The results were verified by an analysis of the Wiberg index. The calculated percentage of evolution of the bond involved in the reaction indicates that the  $\text{C}_2\text{-O}_3$  bond breaking occurs before the bond forming  $\text{C}_2\text{-Cl}_{54}$  in the transition state. The value of synchronicity obtained theoretically is 0.80.

We also showed that the isomerization reaction of the  $\alpha$ -chloroglycidic ester produces  $\alpha$ -chloro-pyruvic ester. It is an exothermic reaction and is thermodynamically possible.

## References

1. Martynov V. F., Titov M. I., *Zurnal obshchei Khimii*. 32 (1962) 319.
2. Coutrot P., Combet J. C., Villieras J., *Tetrahedron Lett.* 12 (1971) 1553.
3. Coutrot P., Legris C., *Synthesis*, (1975) 118.
4. Frish M. J and al., Gaussian 09, Gaussian Inc, Wallingford CT (2009).
5. Dennington R., Keith T., Milam J., Gauss View, Version 5, Semichem Inc., Shawnee Mission, KS, (2009).
6. Becke A. D., *J. Chem. Phys.* 98 (1993) 5648.
7. Perdew J. P., Burke K., *Phys. Rev. Lett.* 77 (1996) 3865.
8. Perdew J. P., *Phys. Rev. B.* 33 (1986) 8822.
9. Dietrichfied R., Hehre W. J., Pople J. A., *J. Chem. Phys.* 54 (1971) 724.
10. Hehre W. J., Dietrichfied R., Pople J. A., *J. Chem. Phys.* 56 (1972) 2257.
11. Hariharan P. C., Pople J. A., *Mol. Phys.* 27 (1974) 209.
12. Gordon M. S., *Chem. Phys. Lett.* 76 (1980) 163.
13. Lee C., Yang W., Parr R.G., *Phys. Rev. B.* 37 (1988) 785.
14. Parr R.G., Yang W., "Density Functional Theory of atoms and Molecules", Oxford University Press, New York (1989).
15. Schlegel H.B., *J. Comput. Chem.* 3 (1982) 214.
16. Schlegel H.B., "Geometry optimization on potential energy surface", in: D.R. Yarkony (ed.), *Modern Electronic Structure Theory*, World Scientific, Singapore, (1994).
17. Marakchi k., Kabbaj O.K., Komihana N., *Journal of fluorine Chemistry*. 114 (2002) 81.
18. Marakchi k., Abou El Makarim H., Kabbaj O.K., Komihana N., *Phys. Chem. News.* 52 (2010) 129.
19. Gonzalez C., Schlegel H.B., "An improved Algorithm for reaction path following", *J. Chem. Phys.* 94 (1989) 2154.
20. Gonzalez C., Schlegel H.B., "An improved Algorithm for reaction path following in mass weighted internal coordinate", *J. Chem. Phys.* 94 (1990) 5523.
21. Domingo L. R., Perez. P., "A DFT study of the ionic [2+2] cycloadditions reactions of keteniminium cations with terminal acetylenes". *Tetrahedron*. 71 (2015) 2421.
22. Cancès M. T., Mennucci V., Tomasi J., *J. Chem. Phys.* 107 (1997) 3032.
23. Cossi M., Barone V., Cammi R. Tomasi J., *J. Chem. Phys. Lett.* 25 (1996) 5327.
24. Barone V., Cossi M., Tomasi J., *J. Comput. Chem.* 19, (1998) 404.
25. Tomasi J., Persico M., *Chem. Rev.* 94 (1994) 2027.

26. Simkin B.Y., Sheikhet I., "Quantum Chemical and statistical Theory of Solutions - A Computational approach", Ellis Horwood: London, UK, (1995).
27. Domingo L., José Aurell M., Jalal R., Esseffar M., Computational and theoretical Chemistry. 6 (2012) 986.
28. Domingo L., Benchouk W., MeKelleche M., *Tetrahedron*. 63 (2007) 4464.
29. Domingo L. R., Teresa Picher M., *Tetrahedron*. 60 (2004) 5053.
30. Sustman R., Sicking W., *J. Am. Chem. Soc.* 118 (1996) 12562.
31. Suarez D., Sordo J.A., *Chem. Commun* (1998) 385.
32. Rodriguez-Otero J., Cabaleiro Lago E.M., *J. Phys. Chem. A* 107 (2003) 1651.
33. Wiberg K.R., *Tetrahedron*, 24 (1968) 1083.
34. Moyano, A., Pericas M. A, Valenti E., *J. Org. Chem.* 54 (1989) 573.
35. Tabyaoui M., "Etude de Méthodologies Originales de Synthèse en Série Glucidique, Dérivées de la réaction de Darzens, et visant la Préparation d'Inhibiteurs Spécifiques de la CMP, KDO Synthétase", Thèse, Nancy I (France), (1993).
36. Hammond, G. S., *J. Am. Chem. Soc.*, 77 (1955) 334.

(2017) ; <http://www.jmaterenvironsci.com>